Phenol transformation and dimerisation, photosensitised by the triplet state of 1-nitronaphthalene: A possible pathway to humic-like substances (HULIS) in atmospheric waters

Phenol transformation and dimerisation, photosensitised by the triplet state of 1-nitronaphthalene: A possible pathway to humic-like substances (HULIS) in atmospheric waters.

Elisa De Laurentiis,[a] Babita Sur,[a,b] Marco Pazzi,[a] Valter Maurino,[a] Claudio Minero,[a] Gilles Mailhot,[c,d] Marcello Brigante,[c,d,*] Davide Vione[a,e,*]

[a] *Dipartimento di Chimica, Università di Torino, Via P. Giuria 5, 10125 Torino, Italy. http://www.chimicadellambiente.unito.it*

[b] *Department of Chemical Engineering, Calcutta University, 92 Acharya P. C. Road, Kolkata 700009, India.*

[c] *Clermont Université, Université Blaise Pascal, Institut de Chimie de Clermont-Ferrand, BP 10448, F-63000 Clermont-Ferrand (France)*

[d] *CNRS, UMR 6296, ICCF, BP 80026, F-63177 Aubière*

[e] *Centro Interdipartimentale NatRisk, Università di Torino, Via L. Da Vinci 44, 10095 Grugliasco (TO), Italy. http://www.natrisk.org*

* Address correspondence to either author. E-mail: marcello.brigante@univ-bpclermont.fr; davide.vione@unito.it

Abstract

The nitroderivatives of polycyclic aromatic hydrocarbons are potentially important photosensitisers in the atmospheric condensed phase. Here we show that the triplet state of 1-nitronaphthalene (^{3}1NN*) is able to directly react with phenol, causing its transformation upon irradiation of 1NN in aqueous solution. Additional but less important processes of phenol degradation are reactions with $^{\bullet}$OH and $^1O_2$, both photogenerated by irradiated 1NN. Dihydroxybiphenyls and phenoxyphenols were detected as main phenol transformation intermediates, likely formed by dimerisation of phenoxy radicals that would be produced upon phenol oxidation by ^{3}1NN*. Very interestingly, irradiation with 1NN shifted the fluorescence peaks of phenol (Ex/Em = 220-230/280-320 nm and 250-275/280-320 nm, with Ex/Em = excitation and emission wavelengths) to a region that overlaps with "M-like" fulvic substances (Ex/Em = 250-300/330-400 nm). Moreover, at longer irradiation times a further peak appeared (Ex/Em = 300-450/400-450 nm), which is in the region of HULIS fluorescence. Irradiated material was also able to photoproduce $^1O_2$, thus showing photosensitisation properties. Therefore, compounds with fluorescence properties that closely resemble those of HULIS (they would be identified as HULIS by fluorescence if present in environmental samples) can be formed upon triplet-sensitised transformation of phenol by 1NN.

Keywords: photoinduced transformation; singlet oxygen; phenoxy radical; kinetic modelling.

1. *Introduction*

Photosensitised reactions involving phenolic compounds in the atmospheric condensed phase have recently gained considerable attention, as a potential source of humic-like substances (HULIS) (Net et al., 2010 and 2011). HULIS are secondary atmospheric constituents (El Haddad et al., 2011) and account for an important fraction of the organic aerosol mass (Decesari et al., 2001). They significantly absorb sunlight, especially at shorter wavelengths (Hoffer et al., 2006), and would play an important atmospheric role as cloud condensation nuclei (Dinar et al., 2007; Wex et al., 2008).

Phenolic compounds may occur in the atmosphere as primary pollutants because of biomass burning (Kuo et al., 2011; Shakya et al., 2011). As secondary pollutants, they derive from $^{\bullet}$OH-induced oxidation of aromatic hydrocarbons emitted by combustion processes (Volkamer et al., 2002). Among the hypothesised pathways of HULIS formation, one involves oxidation of phenols to phenoxy radicals (Net et al., 2011), which yield phenol dimers upon dimerisation and H-atom rearrangement (Neta and Grodkowski, 2005; Sun et al., 2010). Dimers can follow similar reaction pathways until higher oligomers are formed (Net et al., 2010).

Atmospheric photosensitisers include a wide range of compounds with different structures. Common functionalities are aromatic carbonyls including benzophenone-like compounds, antraquinones and aromatic nitroderivatives (Jammoul et al., 2009; Maurino et al., 2011). Brigante et al. (2010) have shown that 1-nitronaphthalene (1NN) is a potentially important photosensitiser, which forms a very reactive triplet state (^{3}1NN*) with high yield.

Interestingly, photosensitised processes in gas-solid systems usually need O_3 for the reaction to proceed (Net et al., 2009 and 2010; Nieto-Gligorovski et al., 2010; Styler et al., 2009 and 2011), while O_3 is not required in aqueous systems (Maddigapu et al., 2011; Maurino et al., 2011). The difference might be due to far easier contact of reactants in aqueous solution.

We here investigate the transformation of phenol in solution (proxy of the atmospheric aqueous phase), photosensitised by 1NN. The reaction was studied by laser flash photolysis (LFP) to assess the reactivity of ^{3}1NN* toward dissolved species. Moreover, steady irradiation experiments were carried out and a kinetic model developed to account for results. Key input data for the kinetic model were obtained by LFP. The potential for phenol to act as HULIS precursor under the studied conditions was assessed by identification of its main phototransformation intermediates. Moreover, fluorescence spectroscopy (excitation-emission matrix, EEM; Muller et al., 2008) was used to monitor a possible shift of fluorescence bands into the HULIS region as irradiation progressed. Photogeneration of singlet oxygen ($^1O_2$), by material formed upon prolonged irradiation of phenol + 1NN, was assessed with furfuryl alcohol (FFA) as $^1O_2$ probe.

2. *Experimental section*

2.1. Laser flash photolysis experiments. A Nd:YAG laser system instrument (Quanta Ray GCR 130-01) operated at 355 nm (third harmonic) with typical energies of 60 mJ (the single pulse was

~9 ns in duration) was used to study the reactions involving the excited state of 1NN (^{3}1NN*). Individual cuvette samples (3 mL volume) were used for a maximum of two consecutive laser shots. The transient absorbance at the pre-selected wavelength was monitored by a detection system consisting of a pulsed xenon lamp (150 W), monochromator and photomultiplier (1P28). A spectrometer control unit was used for synchronising the pulsed light source and programmable shutters with the laser output. The signal from the photomultiplier was digitised by a programmable digital oscilloscope (HP54522A) and analysed by a 32 bits RISC-processor workstation.

Solutions were prepared in Milli-Q water and stability was regularly checked by UV spectroscopy. The decay of ^{3}1NN* and the formation of the radical anion ($1NN^{-\bullet}$) were monitored at 620 and 380 nm. The pseudo-first order decay and growth constants were obtained by fitting the absorbance *vs.* time data with single or double exponential equations. The error was calculated from the scattering of experimental data around the fit function. Experiments were performed at ambient temperature (295±2 °K) on air-equilibrated solutions.

2.2. Irradiation experiments. The samples (5 mL total volume) were placed into cylindrical Pyrex glass cells (4.0 cm diameter, 2.3 cm height) closed with a lateral screw cap, and were magnetically stirred during irradiation. Irradiation was carried out under a Philips TLK 05 UVA lamp, with emission maximum at 365 nm. The incident radiation reached the cells mainly from the top, and the optical path length of the solution was b = 0.4 cm. The lamp irradiance between 300 and 400 nm was 20±2 W m^{-2}, measured with a power meter by CO.FO.ME.GRA. (Milan, Italy). The incident photon flux ((1.6±0.2)·10^{-5} Einstein L^{-1} s^{-1}) was actinometrically determined using the ferrioxalate method (Kuhn et al., 2004), taking into account the absorption spectrum of $Fe(C_2O_4)_3^{3-}$ and the variation with wavelength of the quantum yield of Fe^{2+} generation (Albinet et al., 2010a).

Figure 1 reports the spectral photon flux density over irradiated solutions ($p°(\lambda)$), measured with an Ocean Optics SD 2000 CCD spectrophotometer and normalised to the actinometry results, also taking Pyrex transmittance into account. The Figure also reports the absorption spectrum of 1NN ($\varepsilon_{1NN}(\lambda)$), measured with a Varian Cary 100 Scan UV-Vis spectrophotometer.

2.3. Liquid chromatography determinations. After irradiation the solutions were allowed to cool for 10-15 min under refrigeration, to minimise volatilisation of 1NN. Analysis was then carried out by High Performance Liquid Chromatography coupled with UV-Vis detection (HPLC-UV). The adopted Merck-Hitachi instrument was equipped with AS2000A autosampler (100 μL sample volume), L-6200 and L-6000 pumps for high-pressure gradients, Merck LiChroCART RP-C18 column packed with LiChrospher 100 RP-18 (125 mm × 4.6 mm × 5 μm particle diameter), and L-4200 UV-Vis detector (detection wavelength 220 nm). Isocratic elution was carried out with 60:40 CH_3OH: aqueous H_3PO_4 (pH 2.8), at 1.0 mL min^{-1} flow rate. The retention time of phenol was 2.5 min, that of 1NN 11.2 min, column dead time 0.90 min. FFA analysis was performed using an HPLC system (Waters Alliance) equipped with a diode array detector and a C18 Zorbax column

(Agilent, 15 mm × 4.6 mm × 5 µm). The isocratic eluent was 15:85 CH_3OH:H_2O (1:1000 formic acid) at 1.0 mL min^{-1} flow rate. The retention time of FFA (detected at 220 nm) was 6.5 min.

2.4. Fluorescence measurements. A Varian Cary Eclipse fluorescence spectrofluorimeter was used, adopting a 10 nm bandpass on both excitation and emission. Fluorescence excitation-emission matrix (EMM) was obtained at 5 nm intervals for excitation wavelengths from 200 to 500 nm and emission from 220 to 600 nm. Identification of fluorescent constituents in water samples was performed on the basis of literature data, using the main contours to identify fluorescence peaks.

2.5. Kinetic data treatment. The time evolution data of 1NN and phenol were fitted with pseudo-first order equations of the form $(C_t\ C_o^{-1}) = e^{-k \cdot t}$, where C_t is the concentration of the substrate (1NN or phenol) at time t, C_o its initial concentration, and k (fit variable) the pseudo-first order degradation rate constant. The initial transformation rate is $R = k\ C_o$. Errors on k were derived from the scattering of experimental data around each fit curve. The reported errors on R ($\mu \pm \sigma$) largely depended on k errors, because errors on C_o (derived from calibration curves) were much lower. The reproducibility of repeated runs was around 10-15%. In some cases the experimental rate data were fitted with rather complex equations having one fit variable. The error associated to such variable depended both on data scattering around the fit function and on incertitude of constant parameters, which was taken into account with error propagation rules.

2.6. Identification of transformation intermediates. Intermediate identification was carried out with gas chromatography interfaced with mass spectrometry (GC-MS). Aqueous solutions after irradiation (salted with NaCl and acidified with HCl) were extracted with 3 mL CH_2Cl_2, dehumidified with anhydrous Na_2SO_4 and evaporated to dryness. Each sample was reconstructed with 100 µL CH_2Cl_2. The solution was transferred into a vial and injected into a capillary gas chromatograph (Agilent 6890) coupled with a mass spectrometer (Agilent 5973 inert). The injection system used was a Gerstel CIS4 PTV. Initial injection temperature was 40 °C, programmed at 5 °C/s; final temperature was 320 °C, held for 9 min. The injection volume was 2 µL in the splitless mode. The capillary column used was a HP-5MS, 30 m × 0.25 mm × 0.25 µm film thickness. Initial column temperature was 40 °C and was increased by 15 °C/min to 300 °C. The carrier gas was ultrapure He (flow 1.0 mL min^{-1}; SIAD, Bergamo, Italy). The ionisation source worked in the electronic impact (EI) mode and the mass spectrometer worked in the Scan mode from 44 to 450 Th. Identification of spectra was performed with the Wiley 7n library (Agilent Part No. G1035B).

3. *Results and Discussion*

3.1. Laser flash photolysis (LFP) experiments

LFP runs were carried out to study the reaction between ^{3}1NN* and phenol. Figure 2 reports the absorption spectra obtained, 65 ns after the laser pulse, upon 355-nm flash photolysis of 0.1 mM 1NN (1), of 0.1 mM 1NN + 1 mM phenol (2), as well as the difference spectrum ((2)-(1)). The difference spectrum shows a maximum at 380 nm, where both phenoxy radical (phenoxyl) and $1NN^{-\bullet}$ have absorption peaks (Gadosy et al., 1999; Brigante et al., 2010). Such a finding suggests formation of at least one of the two species. However, the formation of *e.g.* phenoxyl from phenol would imply a one-electron reduction of ^{3}1NN*, which would yield $1NN^{-\bullet}$ as well (Görner, 2008).

The transient ^{3}1NN* could react with both phenol and ground-state 1NN, in addition to reacting with O_2 to yield $^1O_2$ (Brigante et al., 2010). Figure 3a shows the trend of the pseudo-first order rate constant of ^{3}1NN* disappearance ($k_{^3 1NN^*}$), as a function of phenol concentration. The Stern-Volmer approach (Laws and Contino, 1992) yields $k_{^3 1NN^*} = k_{^3 1NN^*, Phenol}[Phenol] + k^o_{^3 1NN^*}$, where $k_{^3 1NN^*, Phenol}$ is the second-order reaction rate constant between ^{3}1NN* and phenol, and $k^o_{^3 1NN^*}$ is the pseudo-first order rate constant of ^{3}1NN* disappearance in the absence of phenol. Therefore, the value of $k_{^3 1NN^*, Phenol}$ can be obtained as the slope of the line $k_{^3 1NN^*}$ *vs.* [Phenol] (Figure 3a). Linear data fit yielded $k_{^3 1NN^*, Phenol} = (4.5 \pm 0.1) \cdot 10^9$ M^{-1} s^{-1}.

Figure 3b shows the trend of $k_{^3 1NN^*}$ *vs.* [1NN], which suggests that some reaction would take place between ^{3}1NN* and 1NN ground state. It is $k_{^3 1NN^*} = k_{^3 1NN^*, 1NN}[1NN] + k^o_{^3 1NN^*}$, from which the second-order rate constant between ^{3}1NN* and 1NN ($k_{^3 1NN^*, 1NN}$) can be determined as the line slope. One gets $k_{^3 1NN^*, 1NN} = (7.1 \pm 0.9) \cdot 10^8$ M^{-1} s^{-1}. From the line intercept ($k^o_{^3 1NN^*} = (4.97 \pm 0.50) \cdot 10^5$ s^{-1}) one can estimate O_2 concentration (Brigante et al., 2010). The resulting $[O_2] = 0.25 \pm 0.03$ mM is quite reasonable for an aqueous solution in contact with the atmosphere.

3.2. Steady irradiation experiments

3.2.1. Irradiation of 1NN alone

Solutions containing 0.1 mM 1NN were irradiated at the natural pH ~ 6, in presence of air and under nitrogen atmosphere. The relevant transformation rates of 1NN were $R^{air}_{1NN} = (6.31 \pm 0.95) \cdot 10^{-9}\ M\ s^{-1}$ and $R^{N_2}_{1NN} = (9.83 \pm 1.18) \cdot 10^{-9}\ M\ s^{-1}$. There is evidence that around 10% of the direct phototransformation of 0.1 mM 1NN in the presence of air is accounted for by photogenerated $^{\bullet}$OH, probably produced upon water oxidation (Sur et al., 2011). The same process would most likely take place under nitrogen, and the photochemical formation rate of $^{\bullet}$OH by 0.1 mM 1NN under the adopted irradiation conditions would be $R^{1NN}_{^{\bullet}OH} \approx (6.3 \pm 0.9) \cdot 10^{-10}\ M\ s^{-1}$.

Considering that 1NN would scavenge practically all photogenerated $^{\bullet}$OH, the rate of 1NN transformation by $^{\bullet}$OH would be equal to $R^{1NN}_{^{\bullet}OH}$. Therefore, the rates of 1NN transformation not

involving $^{\bullet}$OH would be $(R'_{1NN})_{air}$ = (5.68±1.04)·10^{-9} M s^{-1} and $(R'_{1NN})_{N_2}$ = (9.20±1.27)·10^{-9} M s^{-1} under air and N_2, respectively. When the $^{\bullet}$OH pathway is not considered, the following processes would account for the transformation of irradiated 1NN (ISC: inter-system crossing; $\Phi_{^3 1NN^*}$: Fournier et al., 1997; k_4: this work; k_5: Brigante et al., 2010; k_7: Rodgers and Snowden, 1982):

$1NN \xrightarrow{h\nu, ISC} {}^3 1NN^*$	[$\Phi_{^3 1NN^*} = 0.63$]	(1)
${}^3 1NN^* \rightarrow 1NN$	[k_2]	(2)
${}^3 1NN^* \rightarrow$ Products	[k_3]	(3)
${}^3 1NN^* + 1NN \rightarrow 1NN^{+\bullet} + 1NN^{-\bullet}$	[k_4 = (7.1±0.9)·10^8 M^{-1} s^{-1}]	(4)
${}^3 1NN^* + O_2 \rightarrow 1NN + {}^1O_2$	[k_5 = (1.95±0.05)·10^9 M^{-1} s^{-1}]	(5)
$1NN^{-\bullet} + O_2 \rightarrow 1NN + O_2^{-\bullet}$	[k_6]	(6)
${}^1O_2 \rightarrow O_2$	[k_7 = (2.5±0.5)·10^5 s^{-1}]	(7)
$1NN + {}^1O_2 \rightarrow$ Products	[k_8]	(8)

Brigante et al. (2010) determined $k_2+k_3+k_4\cdot[1NN]$ = (8.0±0.1)·10^4 s^{-1}. Reaction (3) would contribute to the transformation of 1NN. In presence of air, reaction (4) is expected to take part in 1NN disappearance, because of the likely evolution of $1NN^{+\bullet}$ into transformation intermediates, while $1NN^{-\bullet}$ would be recycled back to 1NN by oxygen. Under nitrogen atmosphere, the most likely pathway after reaction (4) (in analogy with the behaviour of anthraquinone-2-sulphonate; Maurino et al., 2008) is recombination between $1NN^{+\bullet}$ and $1NN^{-\bullet}$ to give back 1NN, producing a null cycle.

Although $^{\bullet}$OH photoproduction plays some role in the transformation of 1NN, the fraction of ^{3}1NN* that would be involved in $^{\bullet}$OH generation is negligible (Sur et al., 2011). This also means that only a minor fraction of ^{3}1NN* would be involved into 1NN degradation, the remainder giving back 1NN *via* some process. For this reason, $^{\bullet}$OH production was not considered among the significant ^{3}1NN* sinks in steady-state calculations of [^{3}1NN*]. Under N_2 atmosphere, 1NN transformation would be most likely accounted for by reactions (1-4) followed by recombination between $1NN^{+\bullet}$ and $1NN^{-\bullet}$. In air-equilibrated solutions, reactions (1-8) would apply.

The fact that 1NN transformation is faster under N_2 atmosphere than in air-equilibrated solutions, despite the $1NN^{+\bullet}$ + $1NN^{-\bullet}$ recombination without O_2, would be accounted for by the effective scavenging of ^{3}1NN* by O_2 in reaction (5) (Brigante et al., 2010). The process yields $^1O_2$ that contributes to 1NN transformation (reaction (8)), but most $^1O_2$ would actually undergo inactivation in reaction (7). Because [O_2] ~ 0.3 mM, as per its solubility in air-equilibrated solutions and [1NN] = 0.1 mM, the rate of reaction (5) would be ~ 8 times higher than that of reaction (4). Reaction (5) would act as a very effective quenching process for ^{3}1NN*, inhibiting reactions (3) and (4) and decreasing 1NN transformation rate in the presence of oxygen.

The formation rate of ^{3}1NN* can be calculated as $R_{^3 1NN^*} = \Phi_{^3 1NN^*} \cdot P_a^{1NN}$, where $P_a^{1NN} = \int_{\lambda} p°(\lambda)(1-10^{-\varepsilon_{1NN}(\lambda)\cdot b\cdot[1NN]})\,d\lambda$ = (2.5±0.3)·10^{-6} Einstein L^{-1} s^{-1} with b = 0.4 cm and [1NN] = 0.1 mM. Values of $p°(\lambda)$ and $\varepsilon_{1NN}(\lambda)$ are reported in Figure 1. By applying the steady-state

approximation to ^{3}1NN* in the reaction system relevant to nitrogen atmosphere, one gets $(R'_{1NN})_{N_2} = R_{^3 1NN^*} \frac{k_3}{k_2 + k_3 + k_4[1NN]}$. Considering that $R_{^3 1NN^*} = \Phi_{^3 1NN^*} P_a^{1NN} = (1.6 \pm 0.2) \cdot 10^{-6}\ M\ s^{-1}$ and $(R'_{1NN})_{N_2}$ = (9.20±1.27)·10^{-9} M s^{-1} (from irradiation experiments), one obtains k_3 = (4.6±1.3)·10^2 s^{-1}.

In the presence of air, by applying the steady-state approximation to ^{3}1NN* and ^{1}O$_2$ one gets:

$$(R'_{1NN})_{air} = R_{^3 1NN^*} \frac{k_3 k_7 + k_3 k_8 [1NN] + k_5 k_8 [O_2][1NN]}{(k_2 + k_3 + k_4[1NN] + k_5[O_2])(k_7 + k_8[1NN])} \qquad (9)$$

where $(R'_{1NN})_{air}$ = (5.68±1.04)·10^{-9} M s^{-1}. With the value k_3 = (4.6±1.3)·10^2 s^{-1} obtained above, one gets k_8 = (8.1±3.5)·10^6 M^{-1} s^{-1} as the reaction rate constant between 1NN and ^{1}O$_2$. Under such circumstances, only ~0.3% ^{1}O$_2$ would be involved into 1NN transformation in reaction (8), the remainder undergoing thermal inactivation in reaction (7).

3.2.2. Irradiation of 1NN with phenol (air-equilibrated solutions)

Figure 4 reports the trends of the initial transformation rates of 1NN (R_{1NN}) and phenol (R_{Phenol}), as a function of phenol concentration. The direct photolysis of phenol was negligible when it was irradiated alone. The Figure shows that phenol inhibits the transformation of 1NN, which suggests that the two compounds compete for one or more reactive species. In the presence of air, irradiation of 1NN + phenol (PhOH) would involve reactions (1-8) plus the following, where PhO$^\bullet$ is the phenoxy radical (Machado and Boule, 1995; Mark et al., 1996). The constant k_{10} was obtained by LFP (Figure 3a) and k_{13} is reported by Mártire et al. (1993):

^{3}1NN* + PhOH → 1NN$^{-\bullet}$ + PhO$^\bullet$ + H$^+$	[k_{10} = (4.5±0.1)·10^9 M^{-1} s^{-1}]	(10)
PhO$^\bullet$ → PhOH	[k_{11}]	(11)
PhO$^\bullet$ → Products	[k_{12}]	(12)
PhOH + ^{1}O$_2$ → Products	[k_{13} = (1.3±0.3)·10^6 M^{-1} s^{-1}]	(13)

Reactions (11, 12) are pseudo-first order approximations of more complex processes. Rationale for the approximation is to obtain manageable solutions of kinetic equations. For instance, reaction (11) would most likely involve PhO$^\bullet$ + O$_2^{-\bullet}$ (the latter produced in reaction (6)) to give back phenol (Mack and Bolton, 1999; Vione et al., 2011). Formal inclusion of O$_2^{-\bullet}$ in the reaction system would introduce quadratic terms, which would prevent solution of the already complex kinetic equations.

Phenol and 1NN would compete for $^\bullet$OH, which is photogenerated by 1NN with $R_{^\bullet OH}^{1NN} \approx (6.3 \pm 0.9) \cdot 10^{-10}\ M\ s^{-1}$ as estimated before. The reaction rate constants with $^\bullet$OH of phenol and 1NN are $k_{^\bullet OH, Phenol}$ = (1.4±0.1)·10^{10} M^{-1} s^{-1} (Buxton et al., 1988) and $k_{^\bullet OH, 1NN}$ = (8.2±0.4)·10^7 M^{-1} s^{-1} (Sur et al., 2011). The kinetic system made up of equations (1-8) and (10-13), plus $^\bullet$OH-related processes qualitatively predicts inhibition by phenol of 1NN phototransformation, as

actually observed (Figure 4). However, the relevant calculations overestimate the effect of phenol concentration on 1NN degradation rate: experimental data show that inhibition of 1NN degradation by phenol is significantly lower than predicted. The key point is that reaction (10) transforms ^{3}1NN* into 1NN$^{-\bullet}$, which is recycled back to 1NN by O_2 in reaction (6). In this way, the ^{3}1NN*-assisted transformation of 1NN upon reactions (3,4,5,8) is inhibited. To account for experimental data, one should assume that a fraction α of 1NN$^{-\bullet}$ reacts with phenol-derived species to produce transformation intermediates, instead of giving back 1NN. By applying the steady-state approximation to $^\bullet$OH, ^{3}1NN* and $^1O_2$, one gets the following expressions for R_{1NN} and R_{Phenol}:

$$R_{1NN} = R_{^3 1NN^*} \frac{(k_3 + \alpha k_{10}[Phenol])(k_7 + k_8[1NN] + k_{13}[Phenol]) + k_5 k_8 [O_2][1NN]}{(k_2 + k_3 + k_4[1NN] + k_5[O_2] + k_{10}[Phenol])(k_7 + k_8[1NN])} + R_{^\bullet OH}^{1NN} \frac{k_{^\bullet OH,1NN}[1NN]}{k_{^\bullet OH,Phenol}[Phenol] + k_{^\bullet OH,1NN}[1NN]} \quad (14)$$

$$R_{Phenol} = R_{^3 1NN^*} \frac{[k_{12}(k_{11} + k_{12})^{-1} k_{10}[Phenol](k_7 + k_8[1NN] + k_{13}[Phenol])] + k_5 k_{13}[O_2][Phenol]}{(k_2 + k_3 + k_4[1NN] + k_5[O_2] + k_{10}[Phenol])(k_7 + k_8[1NN] + k_{13}[Phenol])} + \quad (15)$$

$$+ R_{^\bullet OH}^{1NN} \frac{k_{^\bullet OH,Phenol}[Phenol]}{k_{^\bullet OH,Phenol}[Phenol] + k_{^\bullet OH,1NN}[1NN]}$$

The fit with equation (14) of the R_{1NN} data reported in Figure 4, with α as the only floating variable, yielded $\alpha = (1.5 \pm 1.3) \cdot 10^{-3}$. This means that <0.3% of 1NN$^{-\bullet}$ would evolve into transformation intermediates, the remainder being recycled back to 1NN by oxygen. The fit with equation (15) of the R_{Phenol} data of Figure 4, with $\beta = k_{12}(k_{11} + k_{12})^{-1}$ as the only floating variable yielded $\beta = (6.8 \pm 3.4) \cdot 10^{-2}$. This means that ≤10% PhO$^\bullet$ would evolve into transformation intermediates, the remainder yielding back phenol (reaction 11).

The good agreement between experimental data and model predictions (Figure 4) suggests that both 1NN and phenol would undergo transformation *via* ^{3}1NN*, $^1O_2$ and $^\bullet$OH. The scavenging of ^{3}1NN* by phenol (reaction 10) would account for most of phenol sensitised transformation, and it would inhibit the degradation of 1NN. The latter issue applies because over 99% of 1NN$^{-\bullet}$ produced in reaction (10) would be recycled back to 1NN by O_2. In the absence of reaction (10), ^{3}1NN* would be involved in 1NN transformation *via* reactions (3,4,5,8).

3.3. Transformation intermediates

Several important transformation intermediates of phenol could be detected by GC-MS. Figure 5 shows their mass spectra and reports comparison with library spectra (match >90%). The relevant intermediates are 2- and 4-phenoxyphenol, 1,1'-dihydroxybiphenyl, and 4,4'-dihydroxybiphenyl. These compounds would arise upon dimerisation of PhO$^\bullet$ (Gopalan and Savage 1994; Platz et al., 1998; Neta and Grodkowski, 2005), produced in reaction (10). The dimerisation rate is expected to increase with increasing phenol concentration (Maurino et al., 2008) and, coherently, GC-MS peaks of intermediates were considerably higher at 1 mM than at 0.1 mM phenol. Note that such concentration values are somewhat higher than the levels of phenolic compounds in fog water (up

to 30 µM, Harrison et al., 2005), but they are in the range of concentrations that phenols can reach in dew water (Polkowska et al., 2008) or in particles from biomass burning (Vicente et al., 2012).

Considering that most of the electron density of $PhO^{\bullet}$ would be localised at the oxygen atom and at the *ortho* and *para* carbon atoms of the ring (Fehir and McCusker, 2009), the structure of the identified intermediates can be easily accounted for. The phenoxyphenols would be formed by addition of the O atom of $PhO^{\bullet}$ to the electron-rich (*i.e.*, 2- and 4-) ring positions of another $PhO^{\bullet}$. The dihydroxybiphenyls would result from an addition process, involving the #2 and #4 ring C atoms of $PhO^{\bullet}$. Further H-atom rearrangement would then yield the detected intermediates.

No transformation intermediates of 1NN were detected. Possible explanations are instability preventing accumulation, poor extraction by CH_2Cl_2, or non-amenability by GC.

3.4. Fluorescence measurements

The variation of fluorescence intensity of solutions upon irradiation was studied by means of the Excitation-Emission Matrix (EEM) technique. Preliminary experiments (data not shown) indicated that 1NN has no fluorescence. Figure 6 reports the EEM spectra of: *(a)* 0.1 mM 1NN + 0.1 mM phenol before irradiation (fluorescence is accounted for by phenol); *(b)* 0.1 mM 1NN + 0.1 mM phenol after 10 min irradiation; *(c)* 0.1 mM 1NN + 0.1 mM phenol after 4 h irradiation, and *(d)* 0.1 mM 4-phenoxyphenol without irradiation. Irradiation of phenol and 1NN shifted the fluorescence emission maximum from ~ 300 nm to 330-400 nm (Figure 6b). Upon prolonged irradiation (4 h) a further, small fluorescence peak appeared at Ex/Em = 300-450/400-450 nm (Figure 6c).

The fluorescence peak of Figure 6b partially overlaps with fluorescence emission by 4-phenoxyphenol (Figure 6d), a transformation intermediate detected in the studied system (see section 3.3), but the fluorescence maximum at Ex/Em = 275/350 nm does not. Substances with Ex/Em = 250-300/330-400 nm would be classified as “M-like” fulvic acids (Parlanti et al., 2000; Mostofa et al., 2011). Moreover, the interval Ex/Em = 300-450/400-450 nm (Figure 6c) is right into the range of atmospheric humic-like substances (HULIS) (Muller et al., 2008). Fluorescence data suggest that irradiation of phenol, in the presence of 1NN as photosensitiser, induces formation of compounds that would be classified as “M-like” fulvic acids and HULIS if found in environmental samples (Muller et al., 2008; Mostofa et al., 2011). The fluorescence of this material only partially overlaps with that of phenol dimer, suggesting that additional and more important fluorescent compounds are being formed. Interestingly, the sensitised phototransformation of 4-phenoxyphenol is known to produce higher oligomers, such as phenol tetramers (Net et al., 2010). Moreover, HULIS formation from phenols might be an important process in the atmosphere, where phenolic compounds arising from wood burning are quite common (Kuo et al., 2011; Shakya et al., 2011).

3.5. Formation of singlet oxygen by the irradiated system 1NN + phenol

Figure 7 reports the time evolution of 1NN, phenol and two fluorescence contours, monitored at Ex/Em = 275/375 nm (fulvic-like) and Ex/Em = 330/415 nm (HULIS), upon irradiation of 0.1 mM 1NN and 60 µM phenol. After 8 h irradiation, phenol and 1NN practically disappeared and "fulvic-like" fluorescence reached a plateau (intensity ~150 A.U.). Fluorescence intensity was remarkably stable in the plateau region, with almost no change at least up to 24 h irradiation. The second fluorescence signal, attributed to HULIS, peaked at around 3 h irradiation (intensity ~ 95 A.U.). The insert of Figure 7 reports the trends up to 2 h irradiation, showing very fast increase of the "fulvic-like" signal.

The material formed after 8 h irradiation was additionally studied for photochemical properties, in particular concerning the ability to produce $^1O_2$. Therefore, 10 µM FFA was added as $^1O_2$ probe to the irradiated system, and FFA degradation was monitored. Figure 8 reports the time trend of 10 µM FFA when irradiated alone (direct photolysis, filled circles), and when it was added to solutions that initially contained 0.1 mM 1NN (empty circles) and 0.1 mM 1NN + 60 µM phenol (triangles). The latter two solutions were both irradiated for 8 h before the FFA spike. The rationale for irradiating FFA alone, or spiked to pre-irradiated 1NN (blank experiments), was to assess direct FFA photolysis and photochemical activity of possible 1NN photointermediates. Indeed, irradiated 1NN is an effective $^1O_2$ source (Brigante et al., 2010), and its (unidentified) intermediates might produce singlet oxygen as well. Note that irradiation of 1NN or FFA alone yielded no fluorescent compounds. Moreover, phenol alone does not absorb above 300 nm, and it did not undergo direct photolysis nor showed fluorescence variation upon irradiation. It was also unable to sensitise FFA transformation.

When FFA was spiked to pre-irradiated 1NN + phenol, its degradation rate was considerably higher compared to blank experiments. Therefore, Figure 8 suggests that the material formed upon irradiation of phenol + 1NN induced photochemical production of $^1O_2$, in addition to showing fluorescence properties analogous to "M-like" fulvic acids and HULIS.

4. *Conclusions*

The triplet state of 1NN reacts with phenol, with rate constant $k_{^3_{1NN^*,Phenol}}$ = (4.5±0.1)·10^9 M^{-1} s^{-1}. The reaction gives phenoxyphenols and dihydroxybiphenyls, coherently with a primary process that would likely produce 1NN$^{-\bullet}$ and the phenoxy radical, PhO$^\bullet$. Note that ≤10% PhO$^\bullet$ is expected to undergo dimerisation, the remainder giving back phenol upon reaction with *e.g.* $O_2^{-\bullet}$. Moreover, 1NN$^{-\bullet}$ would be mostly (>99%) recycled back to 1NN by oxygen. Experimental data are accounted for by a kinetic model made up of reactions (1-8) and (10-13), plus $^\bullet$OH formation by ^{3}1NN* and <0.3% transformation of 1NN$^{-\bullet}$ into intermediates. The majority of phenol would be transformed by ^{3}1NN*, while $^\bullet$OH and $^1O_2$ would play a less important role. Phenol inhibits the transformation of 1NN, because the two substrates compete for reaction with ^{3}1NN*, $^1O_2$ and $^\bullet$OH.

A non-irradiated solution containing phenol and 1NN shows the typical fluorescence emission of phenol. Irradiation causes a red shift of fluorescence excitation and emission wavelengths, from Ex/Em = 220-230/280-320 nm and 250-275/280-320 nm (phenol), to Ex/Em = 250-300/330-400 nm and Ex/Em = 300-450/400-450 nm (contours detected upon irradiation). Compounds with Ex/Em = 250-300/330-400 nm would be identified as "M-like" fulvic substances in environmental samples, while Ex/Em = 300-450/400-450 nm is in the fluorescence range of HULIS. This means that the relevant compounds would be identified as HULIS if found in environmental samples, based on their fluorescence properties. Another interesting finding is that the irradiated material is able to photochemically produce $^1O_2$, thereby showing photosensitisation properties. The potential atmospheric importance of the studied reactions is supported by the fact that both nitroaromatics and phenols are primary and/or secondary atmospheric pollutants, derived from combustion processes. The present work also suggests that EEM fluorescence would be an extremely useful tool to assess the photochemical formation of humic-like and fulvic-like substances.

An issue that deserves further investigation deals with the comparison between humic (or humic-like) substances in the atmosphere *vs*. surface waters. As far as the latter compartment is concerned, photosensitisers such as quinones and aromatic carbonyls can be found in humic and fulvic acids and account for a considerable fraction of their photoactivity (Cory and McKnight, 2005; Canonica et al., 2005; Jammoul et al., 2009; Maurino et al., 2011). There is evidence that atmospheric photosensitisers are less active than those found in surface waters (Albinet et al., 2010b; De Laurentiis et al., 2012). The finding here reported that material with HULIS properties can produce $^1O_2$ when irradiated might give some hints about HULIS photoactivity, and could be scope for further research.

Acknowledgements

DV acknowledges financial support by MIUR – PRIN 2009 (project 20092C7KRC-ARCTICA) and PNRA – Progetto Antartide. The PhD grant of EDL was financially supported by Progetto Lagrange - Fondazione CRT (Torino, Italy). The stay of BS in Torino was supported by Progetto India – Compagnia di San Paolo (Torino, Italy). DV, GM and MB thank EGIDE and Università Italo-Francese (Progetto Galileo) for financial support.

References

Albinet, A., Minero, C., Vione, D., 2010a. Phototransformation processes of 2,4-dinitrophenol, relevant to atmospheric water droplets. Chemosphere 80, 753-758.

Albinet, A., Minero, C., Vione, D., 2010b. Photochemical generation of reactive species upon irradiation of rainwater: Negligible photoreactivity of dissolved organic matter. Science of the Total Environment 408, 3367-3373.

Brigante, M., Charbouillot, T., Vione, D., Mailhot, G., 2010. Photochemistry of 1-nitronaphthalene: A potential source of singlet oxygen and radical species in atmospheric waters. Journal of Physical Chemistry A 114, 2830-2836.

Buxton, G.V., Greenstock, C.L., Helman, W.P., Ross, A.B., 1988. Critical review of rate constants for reactions of hydrated electrons, hydrogen atoms and hydroxyl radicals ($^{\bullet}OH/O^{-\bullet}$) in aqueous solution. Journal of Physical and Chemical Reference Data 17, 1027-1284.

Canonica, S., Kohn, T., Mac, M., Real, F. J., Wirz, J., von Gunten, U., 2005. Photosensitizer method to determine rate constants for the reaction of carbonate radical with organic compounds. Environmental Science & Technology 39, 9182-9188.

Cory, R.M., McKnight, D.M., 2005. Fluorescence spectroscopy reveals ubiquitous presence of oxidized and reduced quinones in dissolved organic matter. Environmental Science & Technology 39, 8142-8149.

De Laurentiis, E., Minella, M., Maurino, V., Minero, C., Brigante, M., Mailhot, G., Vione, D., 2012. Photochemical production of organic matter triplet states in water samples from mountain lakes, located below or above the treeline. Chemosphere 88, 1208-1213.

Decesari, S., Facchini, M.C., Matta, E., Lettini, F., Mircea, M., Fuzzi, S., Tagliavini, E., Putaud, J.P., 2001., Chemical features and seasonal variation of fine aerosol water-soluble organic compounds in the Po Valley, Italy. Atmospheric Environment 35, 3691-3699.

Dinar, E., Taraniuk, I., Graber, E.R., Anttila, T., Mentel, T.F., Rudich, Y., 2007. Hygroscopic growth of atmospheric and model humic-like substances. Journal of Geophysical Research - Atmospheres 112, D05211.

El Haddad, I., Marchand, N., Temime-Roussel, B., Wortham, H., Piot, C., Besombes, J.L., Baduel, C., Voisin, D., Armengaud, A., Jaffrezo, J.L., 2011. Insights into the secondary fraction of the organic aerosol in a Mediterranean urban area: Marseille. Atmospheric Chemistry and Physics 11, 2059-2079.

Fehir, R.J., McCusker, J.K., 2009. Differential polarization of spin and charge density in substituted phenoxy radicals. Journal of Physical Chemistry A 113, 9249–9260.

Fournier, T., Tavender, S.M., Parker, A.W., Scholes, G.D., Phillips, D., 1997. Competitive energy and electron-transfer reactions of the triplet state of 1-nitronaphthalene: A laser flash photolysis and time-resolved resonance Raman study. Journal of Physical Chemistry A 101, 5320-5326.

Gadosy, T. A., Shukla, D., Johnston, L. J., 1999. Generation, characterization and deprotonation of phenol radical cations. Journal of Physical Chemistry A 103, 8834-8839.

Gopalan, S., Savage, P.E., 1994. Reaction mechanism for phenol oxidation in supercritical water. Journal of Physical Chemistry 98, 12646-12652.

Görner, H., 2008. Oxygen uptake after electron transfer from donors to the triplet state of nitronaphthalenes and dinitroaromatic compounds. Journal of Photochemistry and Photobiology A: Chemistry 195, 235-241.

Harrison, M.A.J., Barra, S., Borghesi, D., Vione, D., Arsene, C., Olariu, R.I., 2005. Nitrated phenols in the atmosphere: A review. Atmospheric Environment 39, 231-248.

Hoffer, A., Gelencsér, A., Guyon, P., Kiss, G., Schmid, O., Frank, G.P., Artaxo, P., Andreae, M.O., 2006. Optical properties of humic-like substances (HULIS) in biomass-burning aerosols. Atmospheric Chemistry and Physics 6, 3563-3570.

Jammoul, A., Dumas, S., D'Anna, B., George, C., 2009. Photoinduced oxidation of sea salt halides by aromatic ketones: a source of halogenated radicals. Atmospheric Chemistry and Physics 9, 4229-4237.

Kuhn, H. J., Braslavsky, S. E., Schmidt, R., 2004. Chemical actinometry. Pure and Applied Chemistry 76, 2105-2146.

Kuo, L.J., Louchouarn, P., Herbert, B.E., 2011. Influence of combustion conditions on yields of solvent-extractable anhydrosugars and lignin phenols in chars: Implications for characterizations of biomass combustion residues. Chemosphere 85, 797-805.

Laws, W. R., Contino, P. B., 1992. Fluorescence quenching studies – Analysis of nonlinear Stern-Volmer data. Methods in Enzymology 210, 448-463.

Machado, F., Boule, P., 1995. Photonitration and photonitrosation of phenolic derivatives induced in awueous solution by excitation of nitrite and nitrate ions. Journal of Photochemistry and Photobiology A: Chemistry 86, 73-80.

Mack, J.., Bolton, J.R., 1999. Photochemistry of nitrite and nitrate in aqueous solution: a review. Journal of Photochemistry and Photobiology A: Chemistry 128, 1-13.

Maddigapu, P.R., Minero, C., Maurino, V., Vione, D., Brigante, M., Charbouillot, T., Sarakha, M., Mailhot, G., 2011. Photochemical and photosensitised reactions involving 1-nitronaphthalene and nitrite in aqueous solution. Photochemical & Photobiological Sciences 10, 601-609.

Mark, G., Korth, H.G., Schuchmann, H.P., von Sonntag, C., 1996. The photochemistry of aqueous nitrate ion revisited. Journal of Photochemistry and Photobiology A: Chemistry 101, 89-103.

Maurino, V., Borghesi, D., Vione, D., Minero, C., 2008. Transformation of phenolic compounds upon UVA irradiation of anthraquinone-2-sulphonate. Photochemical & Photobiological Sciences 7, 321-327.

Maurino, V., Bedini, A., Borghesi, D., Vione, D., Minero, C., 2011. Phenol transformation photosensitised by quinoid compounds. Physical Chemistry Chemical Physics 13, 11213-11221.

Mártire, D.O., Evans, C., Bertolotti, S.G., Braslavsky, S.E., García, N.A., 1993. Singlet molecular oxygen [$O_2(^1\Delta_g)$] production and quenching by hydroxybiphenyls. Chemosphere 26, 1691-1701.

Mostofa, K.M.G., Wu, F., Liu, C.Q., Vione, D., Yoshioka, T., Sakugawa, H., Tanoue, E., 2011. Photochemical, microbial and metal complexation behaviour of fluorescent dissolved organic matter in the aquatic environment. Geochemical Journal 45, 235-254.

Muller, C.L., Baker, A., Hutchinson, R., Fairchild, I. J., Kidd, C., 2008. Analysis of rainwater dissolved organic carbon compounds using fluorescence spectrophotometry. Atmospheric Environment 42, 8036-8045.

Net, S., Nieto-Gligorovski, L., Gligorovski, S., Temime-Rousell, B., Barbati, S., Lazarou, Y.G., Wortham, H., 2009. Heterogeneous light-induced ozone processing on the organic coatings in the atmosphere. Atmospheric Environment 43, 1683-1692.

Net, S., Nieto-Gligorovski, L., Gligorovski, S., Wortham, H., 2010. Heterogeneous ozonation kinetics of 4-phenoxyphenol in the presence of photosensitizer. Atmospheric Chemistry and Physics 10, 1545-1554.

Net, S., Alvarez, E.G., Gligorovski, S., Wortham, H., 2011. Heterogeneous reactions of ozone with methoxyphenols, in presence and absence of light. Atmospheric Environment 45, 3007-3014.

Neta, P., Grodkowski, J., 2005. Rate constants for reactions of phenoxyl radicals in solution. Journal of Physical and Chemical Reference Data 34, 109-199.

Nieto-Gligorovski, L.I., Net, S., Gligorovski, S., Wortham, H., Grothe, H., Zetzsch, C., 2010. Spectroscopic study of organic coatings on fine particles, exposed to ozone and simulated sunlight. Atmospheric Environment 44, 5451-5459.

Parlanti, P., Wörz, K., Geoffroy, L., Lamotte, M., 2000. Dissolved organic matter fluorescence spectroscopy as a tool of estimate biological activity in a coastal zone submitted to anthropogenic inputs. Organic Geochemistry 31, 1765-1781.

Platz, J., Nielsen, O.J., Wallington, T.J., Ball, J.C., Hurley, M.D., Straccia, A.M., Schneider, W.F., Sehested, J., 1998. Atmospheric chemistry of the phenoxy radical, $C_6H_5O(\bullet)$: UV spectrum and kinetics of its reaction with NO, NO_2, and O_2. Journal of Physical Chemistry A 102, 7964-7974.

Polkowska, Z., Blas, M., Klimaszewska, K., Sobik, M., Malek, S., Namiesnik, J., 2008. Chemical characterization of dew water collected in different geographic regions of Poland. Sensors 8, 4006-4032.

Rodgers, M.A.J., Snowden, P.T., 1982. Lifetime of $O_2(^1\Delta_g)$ in liquid water as determined by time-resolved infrared luminescence measurements. Journal of the American Chemical Society 104, 5541-5543.

Shakya, K.M., Louchouarn, P., Griffin, R.J., 2011. Lignin-derived phenols in Houston aerosols: Implications for natural background sources. Environmental Science & Technology 45, 8268-8275.

Styler, S.A., Brigante, M., D'Anna, B., George, C., Donaldson, D.J., 2009. Photoenhanced ozone loss on solid pyrene films. Physical Chemistry Chemical Physics 11, 7876-7884.

Styler, S.A., Loiseaux, M.E., Donaldson, D.J., 2011. Substrate effects in the photoenhanced ozonation of pyrene. Atmospheric Chemistry and Physics 11, 1243-1253.

Sun, Y.L., Zhang, Q., Anastasio, C., Sun, J., 2010. Insights into secondary organic aerosol formed via aqueous-phase reactions of phenolic compounds based on high resolution mass spectrometry. Atmospheric Chemistry and Physics 10, 4809-4822.

Sur, B., Rolle, M., Minero, C., Maurino, V., Vione, D., Brigante, M., Mailhot, G., 2011. Formation of hydroxyl radicals by irradiated 1-nitronaphthalene (1NN): Oxidation of hydroxyl ions and water by the 1NN triplet state. Photochemical & Photobiological Sciences 10, 1817-1824.

Vicente, A., Alves, C., Monteiro, C., Nunes, T., Mirante, F., Cerqueira, M., Calvo, A., Pio, C., 2012. Organic speciation of aerosols from wildfires in central Portugal during summer 2009. Atmospheric Environment 57, 186-196.

Vione, D., Sur, B., Dutta, B.K., Maurino, V., Minero, C., 2011. On the effect of 2-propanol on phenol photonitration upon nitrate photolysis. Journal of Photochemistry and Photobiology A: Chemistry 224, 68-70.

Volkamer, R., Klotz, B., Barnes, I., Imamura, T., Wirtz, K., Washida, N., Becker, K.H., Platt, U., 2002. OH-initiated oxidation of benzene - Part I. Phenol formation under atmospheric conditions. Physical Chemistry Chemical Physics 4, 1598-1610.

Wex, H., Stratmann, F., Hennig, T., Hartmann, S., Niedermeier, D., Nilsson, E., Ocskay, R., Rose, D., Salma, I., Ziese, M., 2008. Connecting hygroscopic growth at high humidities to cloud activation for different particle types. Environmental Research Letters 3, 035004.

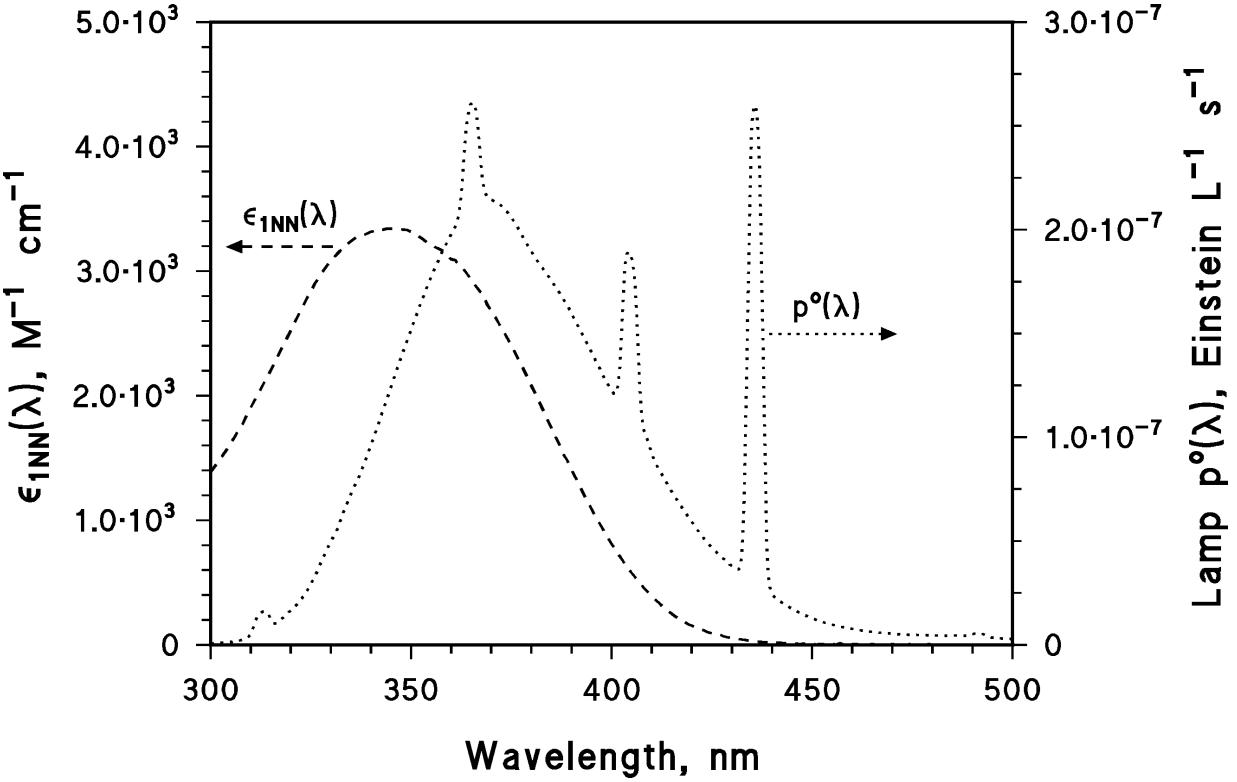

Figure 1. Absorption spectrum (molar absorption coefficient $\varepsilon_{1NN}(\lambda)$) of 1NN. Incident spectral photon flux density ($p°(\lambda)$) of the adopted UVA lamp (Philips TLK 05).

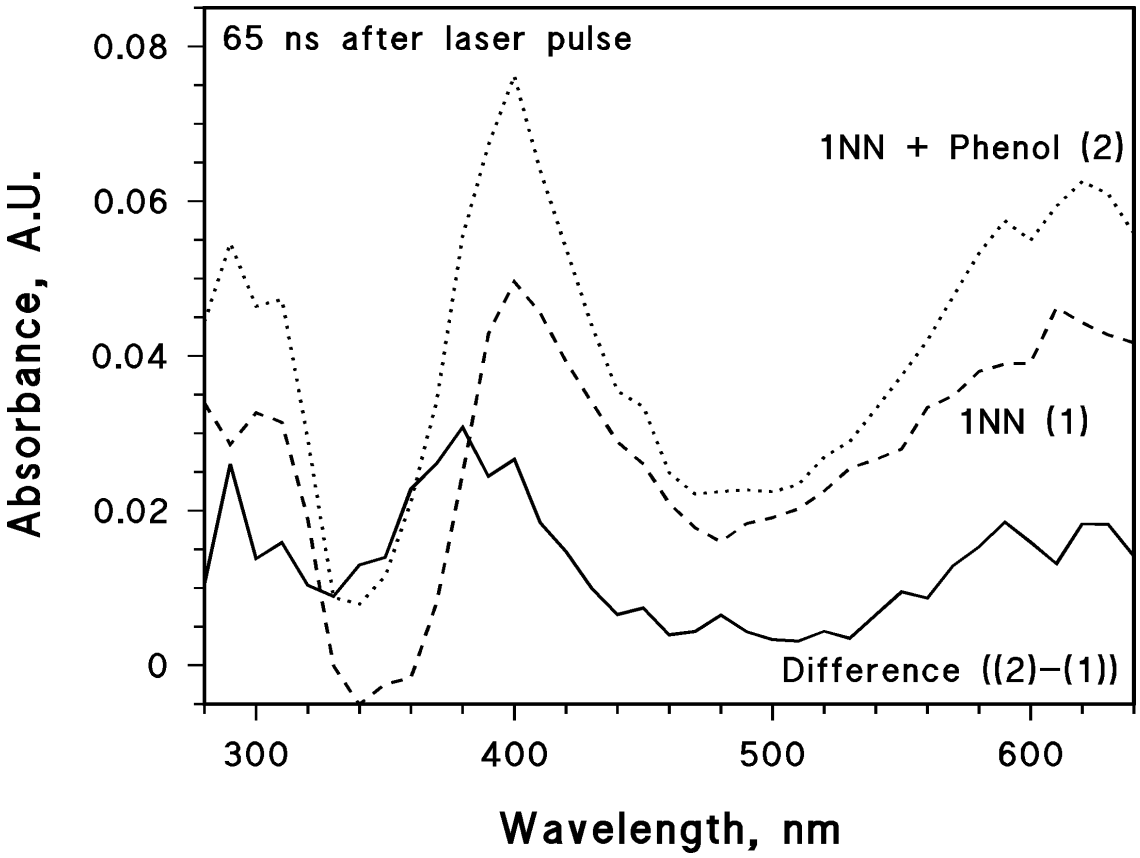

Figure 2. Absorption spectra of transient species formed 65 ns after the laser pulse (355 nm, 60 mJ), upon flash photolysis of air-equilibrated solutions containing: (1) 0.1 mM 1NN; (2) 0.1 mM 1NN + 1 mM phenol. The difference spectrum ((2)-(1)) is also reported.

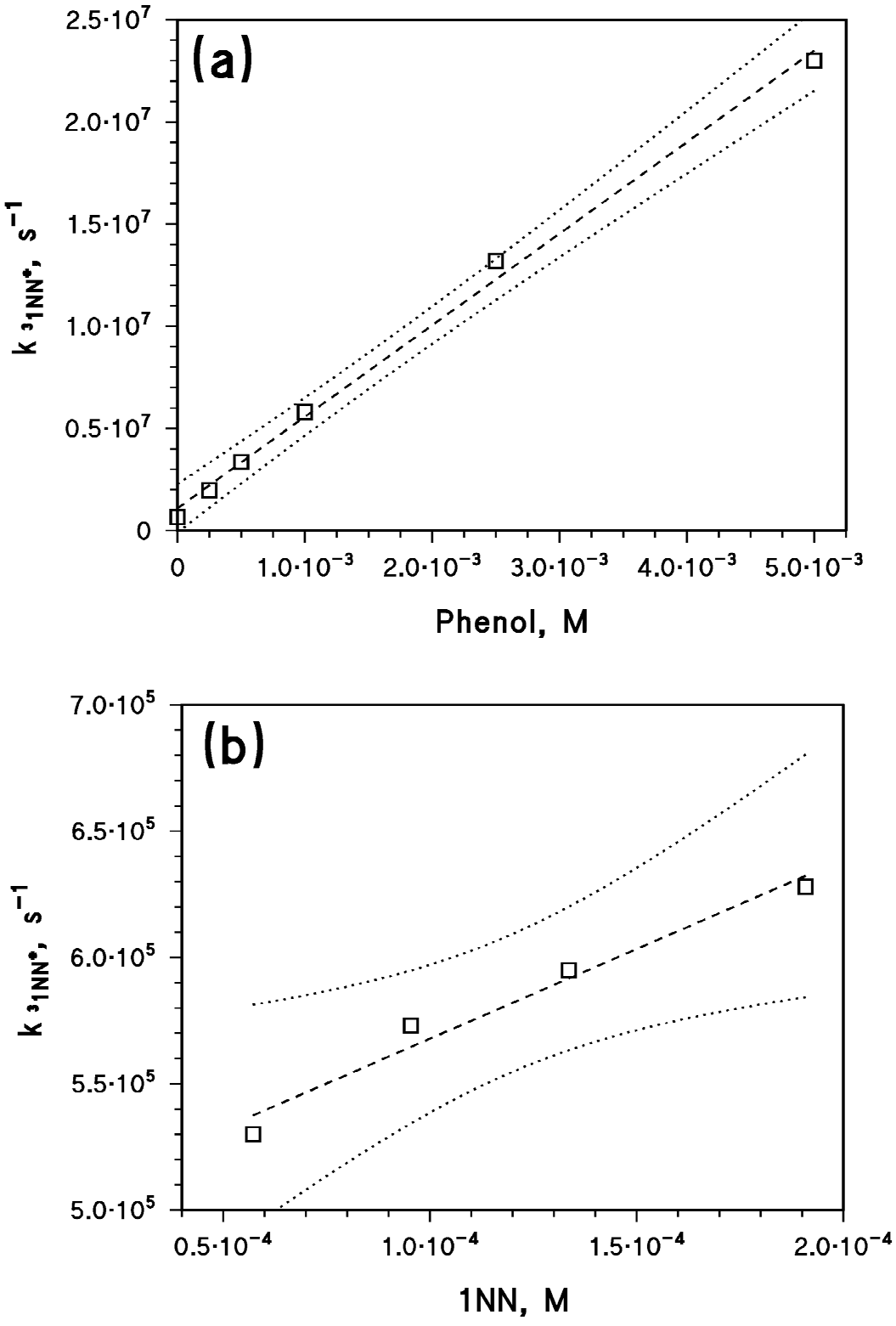

Figure 3. Trend of the first-order rate constant of ^{3}1NN* decay ($k_{^3_{1NN}}$), as a function of **(a)** phenol concentration, and **(b)** concentration of 1NN. Laser pulse: 355 nm, 60 mJ, air-equilibrated solutions.

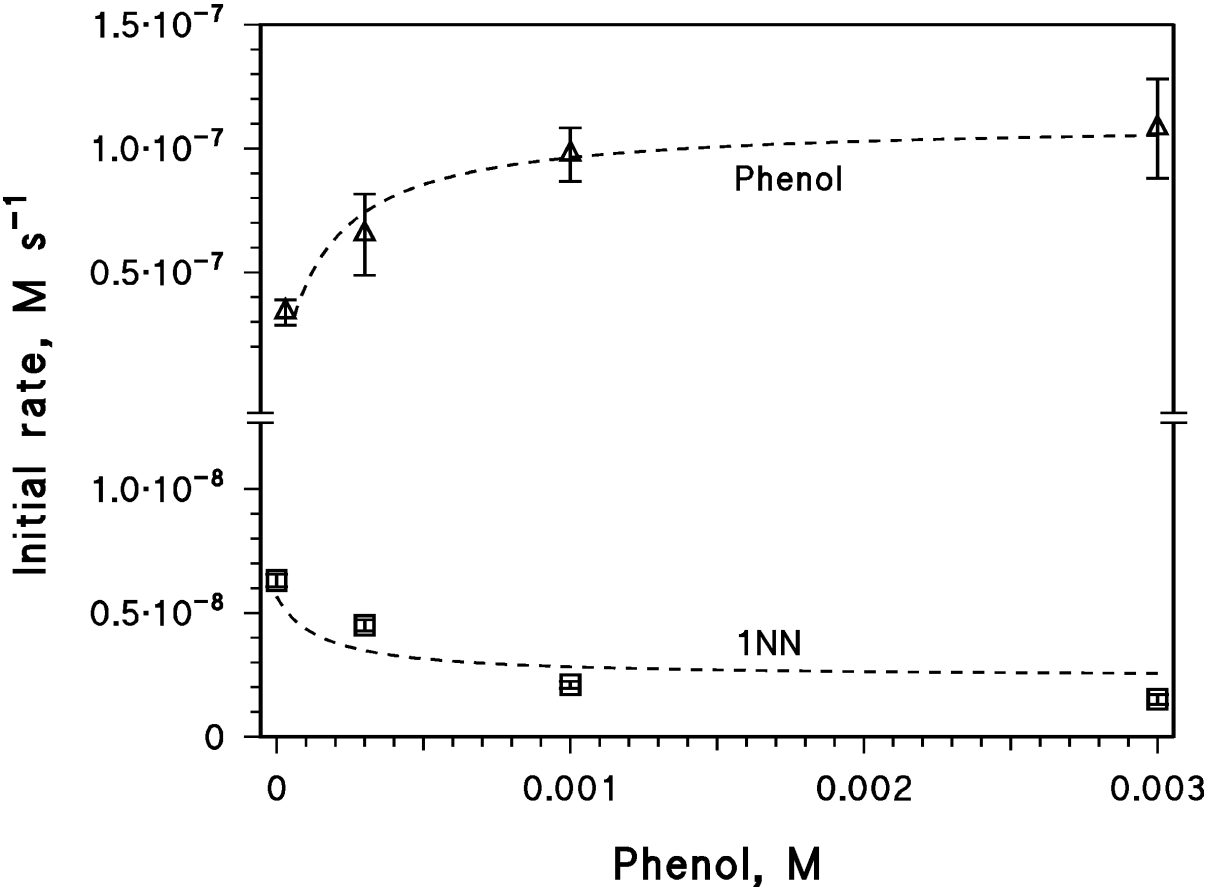

Figure 4. Trend with phenol concentration of the initial transformation rates of phenol and 1NN. The dashed lines are the fit of experimental data with equation (15) (phenol) and equation (14) (1NN). Air-equilibrated solutions, UVA irradiation, pH 6.

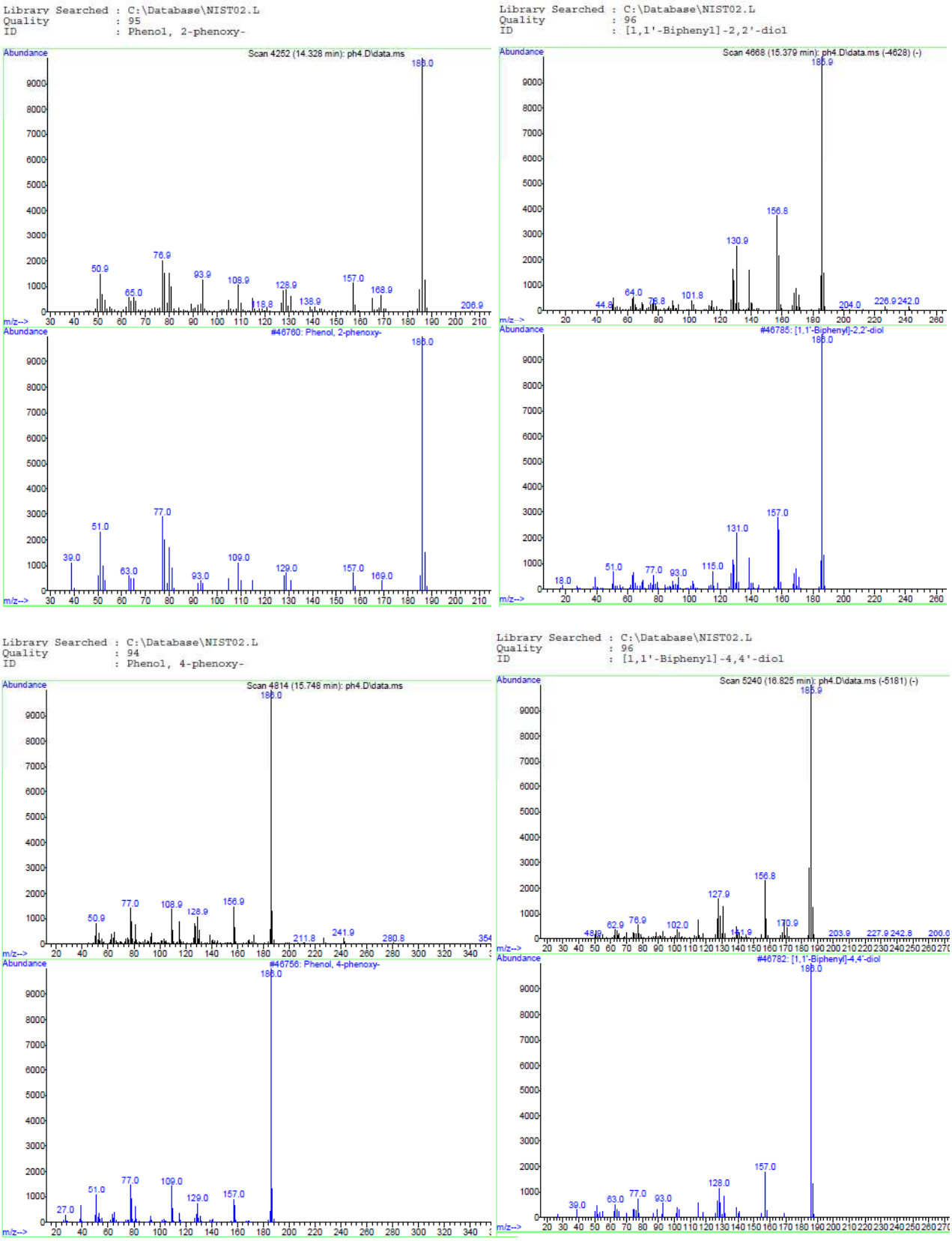

Figure 5. Mass spectra of the detected transformation intermediates (GC-MS analysis). Intermediate structure and library mass spectra are also reported. Peak retention times (minutes) are in brackets over each spectrum.

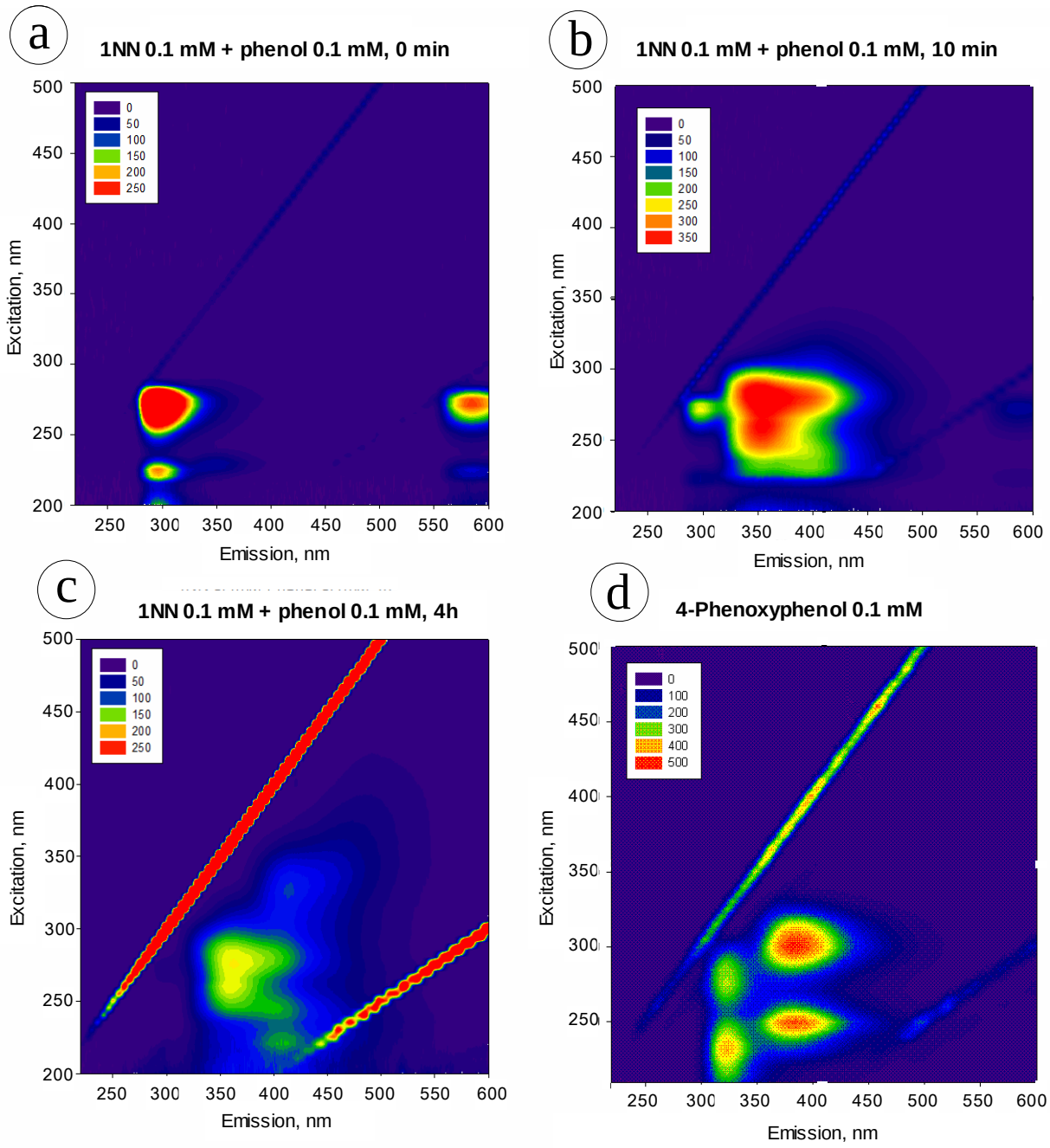

Figure 6. Excitation-Emission Matrix (EEM) fluorescence spectra of: (a) 0.1 mM 1NN + 0.1 mM phenol, before irradiation; (b) 0.1 mM 1NN + 0.1 mM phenol, after 10 min irradiation; (c) 0.1 mM 1NN + 0.1 mM phenol, after 4 h irradiation; (d) 0.1 mM 4-phenoxyphenol.

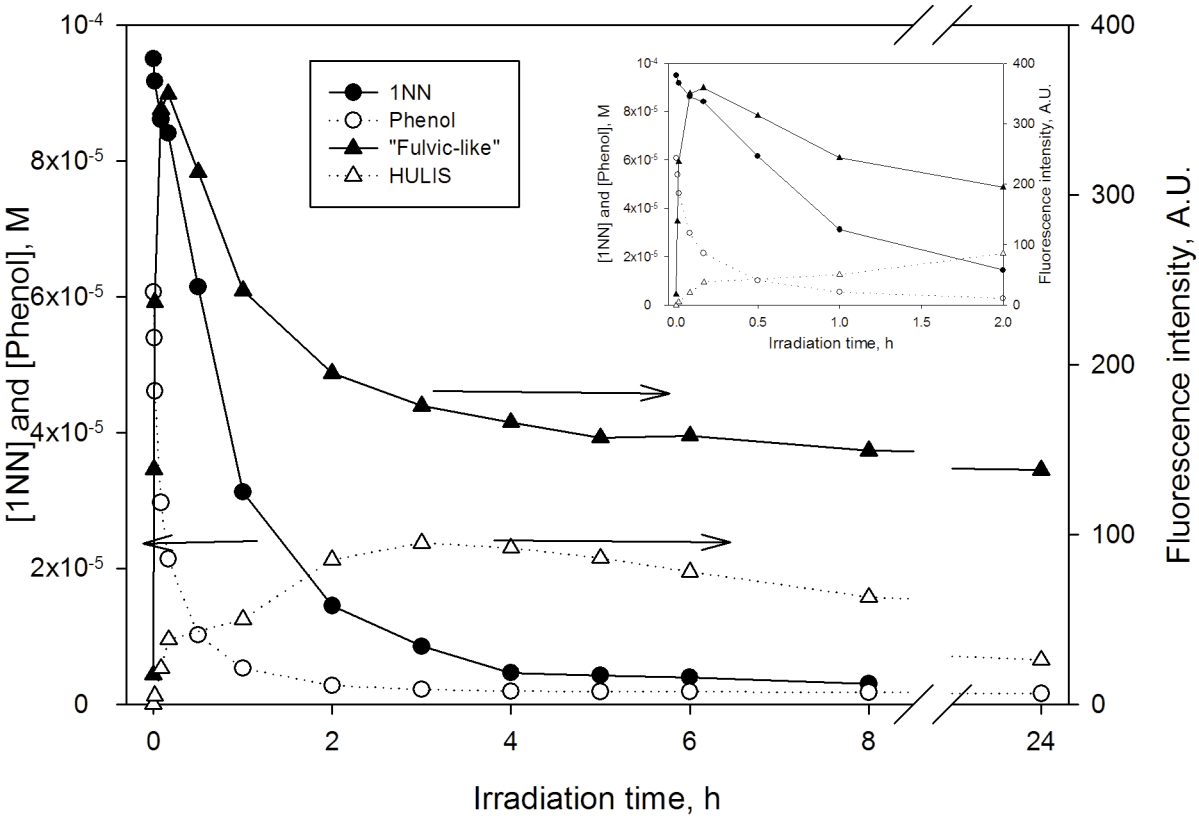

Figure 7. Time trend of 0.1 mM 1NN and 60 µM phenol upon irradiation. Trend of the related intensities of fluorescence, monitored at $\lambda_{Ex,max}$ = 275 nm / $\lambda_{Em,max}$ = 375 nm (Fulvic-like, filled triangles) and at $\lambda_{Ex,max}$ = 330 nm / $\lambda_{Em,max}$ = 415 nm (HULIS, empty triangles). The insert shows the trends from 0 up to 2 hours of irradiation.

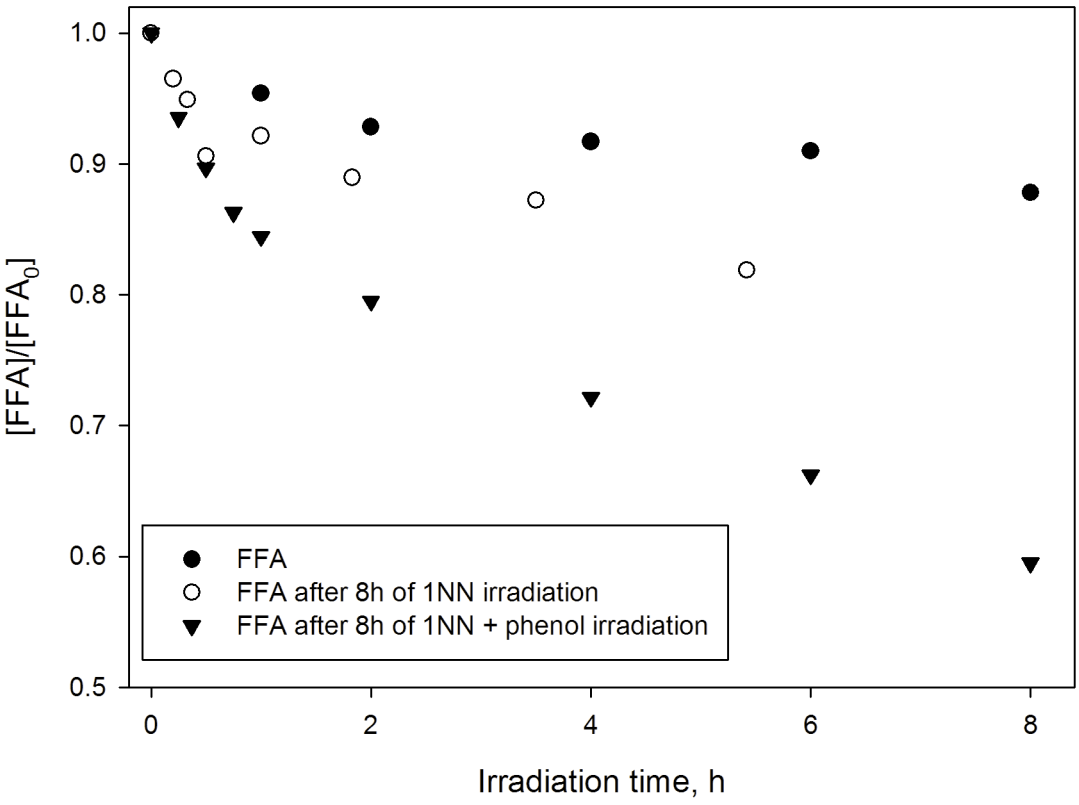

Figure 8. Degradation of 10 µM FFA in Milli-Q water (filled circles), when added to 0.1 mM 1NN solution previously irradiated for 8 h (empty circles), and when added to 0.1 mM 1NN + 60 µM phenol previously irradiated for 8 h (filled triangles).